Hypophosphatemia Due to Increased Effector Cell Metabolic Activity Is Associated with Neurotoxicity Symptoms in CD19-Targeted CAR T-cell Therapy

Jack Pengfei Tang[1], Cole W. Peters[1], Crystal Quiros[1], Xiaoyan Wang[2], Alexandra M. Klomhaus[2], Reiko E. Yamada[3], John M. Timmerman[3,4], Theodore B. Moore[1], and Theodore S. Nowicki[1,4,5,6]

ABSTRACT

A major complication of chimeric antigen receptor (CAR) T-cell therapy is immune effector cell–associated neurotoxicity syndrome (ICANS), which presents as aphasia, confusion, weakness, somnolence, seizures, and coma. This is similar to the neurologic manifestations of hypophosphatemia, which can result from sudden increases in metabolic demand for phosphorylated intermediates (e.g., refeeding syndrome and sepsis). Given these similarities, we investigated whether CAR T-cell effector metabolic activity is associated with increased extracellular phosphate consumption and a possible association between hypophosphatemia and ICANS. *In vitro* 4–1BB and CD28 CD19-targeted CAR T-cell effector activity was found to be associated with increased consumption of media phosphorus, which was temporally associated with increased single-cell effector secretomic activity and increased phosphorus-dependent metabolic demand of the CAR T cells. A clinical cohort of 77 patients treated with CD19-targeted CAR T-cell therapy demonstrated a significant anticorrelation between serum phosphorus and ICANS incidence and severity, with earlier onset of hypophosphatemia after CAR T-cell infusion more likely to result in neurotoxicity. These results imply phosphorous level monitoring could alert to the development of ICANS in clinical scenarios.

See related Spotlight by Tobin et al., p. 1422

Introduction

Chimeric antigen receptor (CAR) T-cell therapy has revolutionized the management of B-cell leukemias and lymphomas. CARs are synthetic receptors composed of an antigen-specific single-chain variable fragment (scFv), hinge, and transmembrane CD3ζ signaling domains, as well as 4-1BB or CD28 costimulatory domains (1). Axicabtagene ciloleucel and tisagenlecleucel are two CD19-targeting CAR T-cell products that were initially approved for relapsed/refractory diffuse large B-cell lymphoma and B-cell acute lymphoblastic leukemia (ALL) in adults and children, respectively (2, 3). Despite their clinical success, CAR T-cell therapies are associated with cytokine release syndrome (CRS) and immune effector cell–associated neurotoxicity syndrome (ICANS). ICANS, which generally presents concomitantly with CRS, manifests as confusion, delirium, aphasia, impaired motor skills, and somnolence. In severe cases, seizures and coma are seen (4–6). Although CRS is managed with targeted therapies that do not inhibit the efficacy of the CAR T cells, such as the anti-IL6 tocilizumab, ICANS management is largely supportive and uses nonspecific immunosuppression with corticosteroids, which may impair CAR T-cell efficacy and therapeutic outcomes (7–10). Thus, the treatment-related morbidity of ICANS presents a need for predictive markers and early interventions.

One clinical anomaly frequently encountered during CAR T-cell therapies or adoptive cell therapies is hypophosphatemia, wherein a patient's serum phosphorus levels are acutely depleted (2, 11, 12). Symptoms of hypophosphatemia, which include weakness, confusion, altered mental status, seizure, and coma, have also been characterized in the context of drastic, acute increases in metabolic demand, as observed with sepsis and refeeding syndrome (13). In such settings, hypophosphatemia results from the redistribution of extracellular phosphorus into cells with acutely increased metabolic demand, due to increased intracellular demand for phosphate for the synthesis of substrates such as ATP, 2-DPG, and CPK (14, 15). Given the striking similarities in the neurologic symptoms of clinical hypophosphatemia and ICANS, as well as the previously characterized widespread incidence of hypophosphatemia during CAR T-cell therapy (2, 11), we investigated whether CAR T-cell engagement with target antigen was associated with increased metabolic activity and extracellular phosphate consumption and whether there was a clinical association of serum hypophosphatemia with ICANS. We found that the increased phosphorus-dependent metabolic demand of CAR T cells, as a consequence of their antigen-directed cytotoxic polyfunctionality, led to the depletion of extracellular phosphorus *in vitro* and that there was a correlation between hypophosphatemia and ICANS during CD19-targeted CAR T-cell therapy in a clinical cohort.

[1]Division of Pediatric Hematology-Oncology, Department of Pediatrics, David Geffen School of Medicine, University of California, Los Angeles, California. [2]Department of General Internal Medicine and Health Services Research, University of California, Los Angeles, California. [3]Division of Hematology-Oncology, Department of Medicine, University of California, Los Angeles, California. [4]Jonsson Comprehensive Cancer Center, University of California, Los Angeles, California. [5]Eli and Edythe Broad Center for Regenerative Medicine and Stem Cell Research, University of California, Los Angeles, California. [6]Department of Microbiology, Immunology, and Molecular Genetics, University of California, Los Angeles, California.

J.P. Tang and C.W. Peters contributed equally to this article.

Corresponding Author: Theodore S. Nowicki, Jonsson Comprehensive Cancer Center (JCCC), University of California, 12-159 Factor Building, 10833 Le Conte Avenue, Los Angeles, CA 90095. Phone: 310-267-5145; Fax: 310-825-2493; E-mail: tnowicki@mednet.ucla.edu

Cancer Immunol Res 2022;10:1433–40

doi: 10.1158/2326-6066.CIR-22-0418

Materials and Methods

Cells

Parental Raji lymphoma cells (ATCC) engineered to express firefly luciferase and GFP were a gift from Yvonne Chen (UCLA) and were cultured in RPMI1640 media (Gibco 11875–093) supplemented with 10% FBS (Sigma F2442), 1xGlutamax (Gibco 35050061), 1xPenecillin/Streptomycin (Thermo 15140122), and passaged every 4 days. Raji-GFP-ffLuc cells were created from Raji cells from ATCC at passage 3. Cells used in our assays were passaged until passage 15 before being discarded (i.e., p1–15+ original p3). Raji cells expressed CD19 and GFP, as observed by flow cytometry and stimulation of CD19-targeted CAR T cells. CD19-targeting human CAR T cells with either 4–1BB–CD28–CD3ζ or CD28–CD3ζ signaling domains and nontargeting (mock) human CAR T with CD28-CD3ζ signaling domain were purchased from Promab Biotechnologies (CAR1000, CAR1001, and CAR1002). CAR T cells were thawed fresh for each assay and recovered overnight in the same media used for the Raji cell culture with the addition of IL2 (10 ng/μL, 300 IU/mL; BioLegend 589104) before use in all coculture assays. All cell cultures were tested for *Mycoplasma* contamination and found negative via the MycoAlert Kit (LT07–318).

Media phosphate uptake assay

For media phosphate uptake assays, RPMI with a physiologic phosphate concentration of 1.45 mmol/L to mimic the phosphate concentration of human sera was created. The medium we started with was RPMI1640 with 0.85 G/L sodium bicarbonate and without L-Glutamine and phosphate (MP Biomedical MP091629754). We supplemented this with sodium phosphate (Fisher S375) to a final concentration of 4.5 mg/dL (w/v), as well as 10% heat-inactivated FBS, 1x penicillin-streptomycin, and 300 IU/mL recombinant human IL2 to resemble our normal CAR T-cell media except with human physiologic phosphate concentration. 4–1BB and CD28 CD19-targeted CAR T cells and mock CAR T cells were cocultured in the physiologic phosphate media with Raji cells at a 10:1 effector:target ratio for 24 and 48 hours, at a final T-cell concentration of 10^6 cells/mL. After coculture, media phosphate was quantified using a colorimetric phosphate kit (Abcam ab65622) and the Varioskan plate reader (Thermo) according to the manufacturer's instructions. Fold increase in phosphate consumption was calculated relative to the mock CAR T-cell coculture.

Cytotoxicity assay

Killing of Raji cells by 4–1BB and CD28 CAR T cells was measured using the Pierce Firefly Luciferase Glow Assay Kit according to the manufacturer's instructions (Thermo 16177). Briefly, 4–1BB, CD28, and mock CAR T cells were cocultured with GFP and luciferase-expressing Raji cells at a 10:1 effector:target ratio for 24 and 48 hours. Cytotoxicity was quantified based on luminescence using a Varioskan Lux plate reader (Thermo) relative to Raji cells alone. Oubain (100 μmol/L, LD90 at 48H; Tocris 1076) was added to Raji cells as a positive control to induce apoptotic cell death.

Analysis of metabolic parameters

Respirometry assays were performed on a Seahorse XF96 Extracellular Flux Analyzer (Agilent Technologies). 4–1BB and CD28 CAR T cells were cultured at a density of 1×10^6 cells/mL in the same complete RPMI media with recombinant human IL2 (20 ng/mL) used for overnight recovery (see *Cells*). After 24 hours, CAR T cells were cocultured with GFP-Luc-Raji cells at a 10:1 effector:target ratio for 24 hours in physiologic phosphate media, prepared as described above (see *Media Phosphate Uptake Assay*). Cells were then seeded at 2×10^5 cells/well in a poly-d-lysine coated Seahorse XF96 microplate and centrifuged to allow for cell adherence to the plate. Cells were plated in Seahorse assay medium [DMEM (Sigma D5030) supplemented with 8 mmol/L glucose (Sigma G5767), 2 mmol/L glutamine (Gibco 25030–081), 1 mmol/L sodium pyruvate (Gibco 11360–070), and 5 mmol/L HEPES (Thermo 15630080); pH 7.4]. The XF96 plate was incubated at 37°C for 45 minutes in an incubator without CO_2 before starting the assay. During the assay, the following modifying agents were introduced: oligomycin (an inhibitor of ATP synthase) (Sigma 495455) was injected from Port A to a final concentration of 2 μmol/L. Carbonyl cyanide-p- trifluoromethoxyphenylhydrazone (FCCP, an uncoupling ionophore; Enzo LS BML-CM10) was injected from Ports B and C to final concentrations of 1 μmol/L and 1.8 μmol/L, respectively. Finally, rotenone (Sigma 557368) and antimycin A (Sigma A8674), which block electron transport chain (ETC) complexes I and III, respectively, were injected from Port D to a final concentration of 2 μmol/L. Measurements of ATP-dependent respiration were made by subtracting the nonmitochondrial linked respiration rate from the measured oxygen consumption rate (OCR) after each of the three steps via the following mechanisms: (i) oligomycin blocks ATP-linked respiration; (ii) FCCP ablates the inner mitochondrial membrane potential, allowing ETC maximal rate; and (iii) the final inhibitors completely degenerate the ETC leaving the nonmitochondrial respiration rate as the ultimate baseline value with which to calculate the respiration rates from each step. Seahorse data were normalized to cell number/well by quantifying Hoechst-stained nuclei. After the assay, cells were stained with 1-μg/mL Hoechst (Thermo 62249) and quantified with an Operetta High-Content Imaging System (PerkinElmer). This approach allowed us to determine the OCR, which measures ATP generation via oxidative phosphorylation, and the extracellular acidification rate (ECAR), which measures ATP generation via glycolysis. Data are presented as pmoles O_2/minute for OCR and mpH/min for ECAR. Data were analyzed by first subtracting nonmitochondrial respiration (lowest rate after injection of antimycin A and rotenone) from all OCRs. Basal OCR and ECAR were calculated as the average of the two measurements before injection of oligomycin. Proton leak was measured as the lowest rate after injection of oligomycin. To determine ATP-linked respiration, proton leak was subtracted from basal respiration. Maximal respiration was calculated as the highest rate after FCCP injections. To determine reserve capacity, basal respiration was subtracted from maximal respiration. ATP production rates from glycolysis and oxidative phosphorylation were calculated as previously described (16).

Analysis of single-cell cytokine secretion

4–1BB and CD28 CAR T cells were cultured at a density of 10^6 cells/mL in complete RPMI media with recombinant human IL2 (20 ng/mL) for overnight recovery. After 24 hours, CAR T cells were cocultured with GFP-Luc-Raji cells at a 10:1 effector:target ratio for 24 hours in physiologic phosphate media. After 24-hour coculture, cells were labeled with membrane stain and loaded into a single-cell 32-plex IsoCode chip (IsoPlexis ISOCODE 1001–4) at a density of 1×10^6 cells/mL according to the manufacturer's instructions. Protein secretions from ∼1,000 single cells were captured by the 32-plex antibody barcoded chip and analyzed by fluorescence ELISA-based assay as previously described (17, 18) on an IsoSpark platform. Polyfunctional CAR T cells (single cells secreting 2 or more cytokines) were evaluated using IsoSpeak software (IsoPlexis) for five functional profiles: (i) effector (granzyme B, perforin, IFNγ,

MIP-1α, TNFα, TNFβ); (ii) stimulatory (GM-CSF, IL2, IL5, IL7, IL8, IL9, IL12, IL15, IL21); (iii) regulatory (IL4, IL10, IL13, IL22, TGFβ, sCD137, sCD40L); (iv) chemoattractive (CCL-11, IP-10, MIP-1β, RANTES); and (v) inflammatory (IL1β, IL6, IL17A, IL17F, MCP-1, MCP-4). The polyfunctional strength index (PSI) of CAR T-cell functional group products was computed using a prespecified formula, defined as the percentage of polyfunctional cells, multiplied by mean fluorescence intensity of the proteins secreted by those cells, as previously described (17, 18).

Retrospective analysis of CD19-targeted CAR T-cell clinical cohort

The study population consisted of 77 patients with B-cell malignancies treated with CD19-targeted CAR T-cell therapy (tisagenlecleucel or axicabtagene ciloleucel) at UCLA between March 2018 and July 2020. All clinical details of patients were retrospectively obtained from the electronic medical record under UCLA Institutional Review Board (IRB) 20–001182, and this was approved by the UCLA IRB in compliance with the U.S. Common Rule and the Belmont Report. The UCLA IRB waived the requirement for informed consent under 45 CFR 46.116 for this research. Clinical details obtained included demographic information (age, sex), infusion product, and clinical diagnosis. Information from daily labs from admission to discharge were also extracted, including serum electrolytes (sodium, potassium, phosphorus, magnesium) and inflammatory markers [C-reactive protein (CRP)]. Hypophosphatemia was defined as serum phosphorus level <2.0 mg/dL; hypokalemia as serum potassium level <3.5 mEq/L; and hypomagnesemia as serum magnesium <1.6 mg/dL; these were also the levels at which electrolyte repletion was indicated per unit standard operating procedures (SOP). Information about CRS and ICANS incidence was extracted from the patients' charts. The severity of CRS was reported on a scale of 1 to 4 (19). Neurotoxicity was reported as an ICANS grade from 1 to 4 with increasing severity of symptoms (19), and a CARTOX-10 score from 1 to 10 with decreasing severity of symptoms (4, 19). These grades were assigned daily by the primary oncology team during hospitalization. Interventions for CRS and/or ICANS, including tocilizumab, dexamethasone, and anakinra were noted. Response to treatment based on follow-up PET/CT, progression-free survival (PFS), and overall survival (OS) were also documented.

Statistical analysis

Baseline demographic characteristics were reported as mean ± SD for normally distributed continuous variables, median and interquartile range for non-normally distributed continuous variables, and count and percentage for categorical variables. Univariable logistic regression was used to determine the association between continuous variables (serum phosphorus, time from cell infusion) and the incidence of ICANS. Fisher exact test was used to characterize the association between categorical variables and the incidence of ICANS. Unpaired Student *t* test was used to compare nadir electrolyte values and peak CRP values between ICANS and non-ICANS groups, as well as *in vitro* cell killing, extracellular phosphate, cytokine secretion polyfunctionality, and SeaHorse assays. Mann–Whitney U test was used to compare time to resolution of ICANS or ICANS severity in those with hypophosphatemia and those with normal values. Time to event data was summarized using the Kaplan–Meier method with surviving patients censored at the date of retrospective chart review or event, with event being death for OS, or disease progression for PFS, and compared using the log-rank test. Linear mixed-effects models were used to assess the temporal relationship between neurotoxicity and serum phosphorus. We defined serum phosphorus measurement as the outcome variable and ICANS (or CARTOX-10) score, time from the first lab assessment, and an interaction between time and score as fixed effects. Individual patients were allowed to have random intercepts to account for variability in baseline measurements. Model-based estimates are presented graphically. We also generated descriptive statistics, including N and relative frequencies of subgroups of patients with ICANS, hypophosphatemia, and severe CRS. To describe the probability of ICANS for patients with severe CRS (defined as grade ≥2) and hypophosphatemia, and account for potential confounding between the conditions, we ran a logistic regression model with ICANS as the dependent variable and included indicators for both severe CRS and hypophosphatemia as independent variables. We report parameter estimates and ORs, and associated *P* values. For all statistical investigation, an alpha/*P* value of <0.05 was used as the cutoff for significance for two-sided statistical testing. Graphing and statistical analyses were performed using GraphPad Prism V.9 (GraphPad), SAS version 9.4 (SAS Institute, Inc.), or R V.4.0.2 using the Readxl tidyverse R package (https://github.com/tidyverse/readxl).

Data availability

The data generated in this study are available within the article and its Supplementary Data files or from the corresponding author upon reasonable request.

Results

Metabolically active CD19-targeted CAR T cells *in vitro* consume extracellular phosphate

To investigate whether hypophosphatemia, as a sequela of CAR T-cell therapy, could be attributed to CAR T-cell activation and target cell killing, we used a coculture system with $CD19^+$ Raji B-cell lymphoma cells expressing firefly luciferase. Coculture of target cells with CAR T cells expressing CD19-targeted CARs linked to intracellular CD3ζ via CD28 or 4–1BB+CD28 costimulatory domains led to robust target cell killing (**Fig. 1A**). Collecting cell-free media from the coculture allowed us to monitor extracellular phosphate concentrations present after cell killing via a colorimetric assay. CD19-targeted CAR T cells cocultured with $CD19^+$ Raji target cells consumed significantly more phosphate than T cells carrying the same CAR constructs cultured alone (1.59-fold more) or than mock CAR T cells, which lacked the target-recognizing scFv domain, cultured with $CD19^+$ Raji target cells (1.53-fold; **Fig. 1B**). Extracellular phosphate levels were not significantly different between Raji cells cultured alone and those cocultured with mock CAR T cells, as well as 4–1BB and CD28 CAR T cells cultured alone. Treatment of Raji cells with the apoptotic agent oubain did not alter extracellular phosphate levels despite cell death rates similar to those observed when Raji cells were cocultured with CAR T cells (**Fig. 1A** and **B**), suggesting that phosphorus consumption was not due to intrinsic differences in CAR T-cell metabolism or target cell death.

To investigate whether differences in antigen-dependent extracellular phosphate consumption between CAR T cells cultured with or without Raji cells were associated with increased cytokinetic functionality, we conducted single-cell cytokine secretion assays (**Fig. 1C**). The assay we used monitors a panel of 32 cytokines from a single-cell flow chamber, yielding a single-cell secretome profile. These parameters were then amalgamated into a single PSI based on secretion levels from single cells, the percentage of the cell population expressing these markers, and the proportion of cells producing two or more cytokines, as previously described (17, 18). This analysis demonstrated

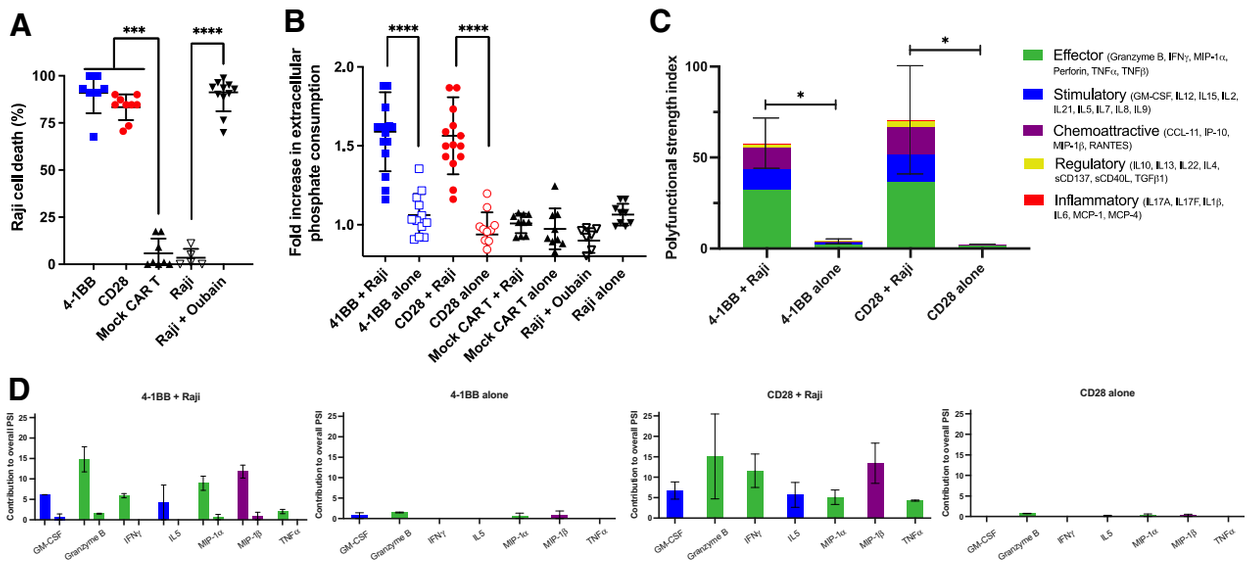

Figure 1.

CD19-targeted CAR T cell–mediated cytotoxicity consumes extracellular phosphate *in vitro*. **A,** Tumor cell lysis during coculture killing assay. 4–1BB and CD28 CD19-targeted CAR T cells were cocultured with CD19$^+$ Luciferase$^+$ Raji tumor cells at a 10:1 effector:target ratio for 48 hours. Raji cells were also cocultured with the pro-apoptotic agent ouabin as a positive control. Cell death was measured via firefly luciferase luminescence compared with non-CD19–targeting mock CAR T cells cocultured with Raji cells ($n = 9$, 3 experiments). **B,** Phosphate content in the media from CAR T cells cultured alone or with CD19$^+$ Raji target cells was quantified using a colorimetric assay and reported as a fold increase in phosphate consumption compared with the mock CAR T-cell coculture (41BB, CD28 CAR T $n = 15$, Mock $n = 10$; 5 experiments). **C,** 32-plex single-cell cytokine secretion profile of CD19-targeted CAR T cells in the presence or absence of Raji cells categorized into domains of cytokinetic polyfunctionality. PSI aggregates all single-cell multidimensional data into a single index, defined as the percentage of polyfunctional cells, multiplied by the sum of the mean fluorescence intensity of the proteins secreted by those cells, which are subdivided into different functional categories of cytokines (effector, stimulatory, chemoattractive, regulatory, and inflammatory cytokines). The aggregate cytokine secretome PSI of T cells bearing either the 41BB or CD28 CD19-targeted CAR constructs were significantly increased in the presence of their target antigen ($n = 3$). **D,** The PSI composition further uncovers GM-CSF, Granzyme B, IFNγ, IL5, MIP-1α, MIP-1β, and TNFα as the major drivers for the increased antigen-driven PSI. Profiles were broken down by cytokine, between functional categories, to reveal the specific proteins driving the PSI. Data are plotted as mean ± SEM. *, $P < 0.05$; ***, $P < 0.001$; ****, $P < 0.0001$; unpaired t test.

that coculturing 4–1BB and CD28 CAR T cells with CD19$^+$ Raji cells significantly increased their effector, stimulatory, and chemoattractive PSI, predominantly as a result of increased amounts of granzyme B, IFNγ, GM-CSF, MIP-1α, MIP-1β, IL5, and TNFα (**Fig. 1C** and **D**). CAR T cells cultured alone and mock CAR T cells cocultured with CD19$^+$ Raji cells demonstrated negligible cytokine secretion. In parallel with the greater observed phosphate depletion of cocultured cells, these observations suggest phosphate consumption increases during T-cell activation due to CAR recognition of antigen.

To investigate the enhanced phosphorus-dependent metabolic requirements of CAR T cells during cell killing as a putative driver of extracellular phosphate consumption, SeaHorse assays were performed on the CAR T cells to determine their cellular OCR and EACR. These metrics indirectly measure phosphate consumption via generation of ATP via oxidative phosphorylation and glycolysis, respectively. After 24 hours of coculture with CD19$^+$ Raji target cells, CD28 CAR T cells demonstrated increased basal OCR compared with mock CAR T cells (**Fig. 2A**). This was also observed for ATP-linked consumption after addition of oligomycin. However, both 4–1BB and CD28 CAR T cells cocultured with CD19$^+$ Raji cells had significantly greater maximal and reserve capacity OCRs than mock CAR T cells cocultured with CD19$^+$ Raji cells, consistent with CAR recognition of cognate antigen driving increased phosphorus-dependent metabolic activity (**Fig. 2A** and **B**). ECAR, a measurable surrogate for lactic acid production during glycolysis, was also higher in both CD28 and 4–1BB CAR T cells during coculture compared with the same CAR T cells cultured alone, or cocultured mock CAR T cells (**Fig. 2A** and **B**). CD28 CAR T cells cultured alone showed a higher ECAR than mock CAR T cells cocultured with CD19$^+$ Raji cells, indicating that the CD28 CAR T cells had a higher intrinsic metabolic rate compared with the 4–1BB CAR T cells. ATP production (normalized to cell number) was also directly calculated, and we observed higher metabolic activity in 4–1BB and CD28 CAR T cells when cocultured with CD19$^+$ Raji target cells as opposed to when they were cultured alone, confirming higher phosphorus-dependent metabolic rate and resource consumption occurs upon CAR T-cell activation with target antigen (**Fig. 2C**). Taken together, these observations indicate that CAR T cell–mediated cell killing requires an uptake in extracellular phosphate, which is temporally associated with ATP-dependent metabolism. Although CD28 CAR T cells exhibited increased basal metabolic activity over the T cells with the 4–1BB construct, this did not translate into meaningful differences in cell killing or cytokinetic polyfunctionality.

Hypophosphatemia correlates with ICANS incidence and severity following CD19-targeted CAR T-cell therapy

Given our observation that extracellular phosphate was depleted *in vitro* in the setting of antigen-directed cell killing by CAR T cells, and the known neurologic impact of clinical hypophosphatemia, we retrospectively examined data from 77 patients treated at the University of California, Los Angeles with CD19-targeted CAR T-cell therapy to determine if serum hypophosphatemia was associated with the onset and severity of ICANS. In our cohort, 23 (30%) patients

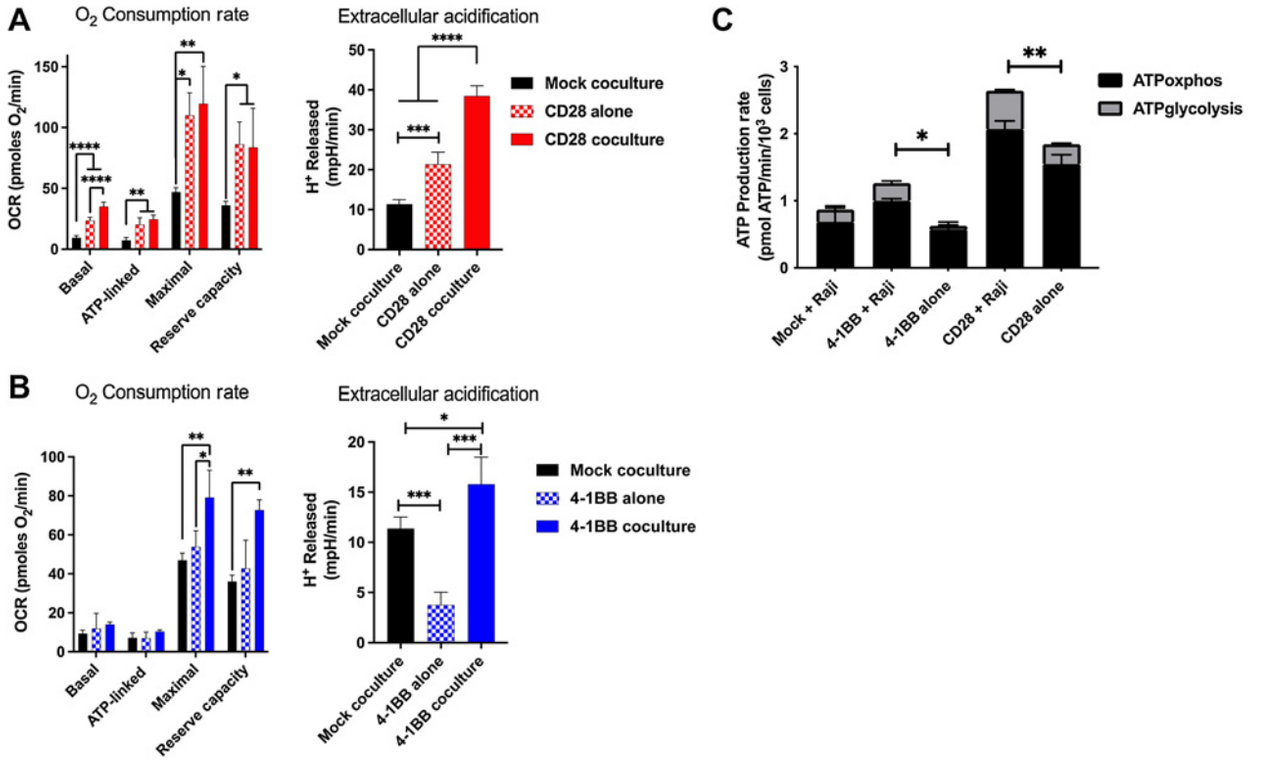

Figure 2.

Target antigen stimulation of CD19-targeted CAR T cells increases phosphorus-driven cellular metabolic demand. Basal, ATP-linked, maximal, and reserve OCR and basal extracellular acidification were measured under basal metabolic conditions and in response to mitochondrial inhibitors, as specified in the methods after 24 hours of coculture of (**A**) CD28 or (**B**) 4-1BB CAR T cells with $CD19^+$ Raji target cells. **C,** ATP production rate from oxidative phosphorylation and glycolysis normalized to cell density. Results are demonstrative of quintuplicate wells during independent experiment. *, $P < 0.05$; **, $P < 0.01$; ***, $P < 0.001$; ****, $P < 0.0001$; unpaired *t* test.

developed ICANS, with a median onset of 5 days post-infusion of CD19-targeted CAR T cells; 86.7% ($N = 17$) of these patients were defined as having severe ICANS, with grade ≥2 (Supplementary Fig. S1A and S1B). Patient characteristics (age, sex), disease characteristics, and infusion product had no significant association with the development of ICANS (**Table 1**). CRS was seen in 69% of patients, including all patients who developed ICANS. Peak values of the acute inflammatory marker CRP were significantly higher in patients who developed ICANS (**Table 1**; **Fig. 3A**).

Serum electrolyte disturbances previously reported in the setting of CAR T-cell therapy (2, 11) were also characterized. In our cohort, 60% of patients had a nadir serum phosphorus in the hypophosphatemic range (<2 mg/dL), 52% had a nadir serum potassium in the hypokalemic range (<3.5 mEq/L), and 72% had a nadir serum magnesium in the hypomagnesemic range (<1.6 mg/dL). Only hypophosphatemia was significantly associated with ICANS ($P = 0.0003$; **Table 1**). The median time to nadir for phosphorus was day five post-infusion of the CD19-targeted CAR T cells, which coincided with the median onset of ICANS, whereas the median time to nadir for potassium and magnesium was on day 2 (**Fig. 3B**). The mean nadir serum phosphorus of the ICANS group was significantly lower than that of the non-ICANS group (1.391 mg/dL vs. 2.130 mg/dL; $P = 0.0002$), while no significant differences in nadir potassium and magnesium were observed (**Fig. 3C**). On an individual patient level, we observed that decreases in serum phosphorus within the threshold for clinical hypophosphatemia coincided with the onset of ICANS (Supplementary Fig. S2). To further characterize the relationship between serum phosphorus and ICANS, a linear mixed-effects model was developed, with serum phosphorus as the outcome variable, and both time from CAR T-cell infusion and ICANS grade/CARTOX-10 score (both measures of neurotoxicity severity) as the fixed effects of the model. Individual patients were allowed to have random intercepts to account for variabilities in baseline values. On the basis of this model, ICANS grade was negatively associated with serum phosphorus, with each unit increase in ICANS grade associated with a 0.29 mg/dL decrease in phosphorus ($P < 0.0001$; **Fig. 3D**). Likewise, CARTOX-10 score was positively associated with serum phosphorus, with each point of reduction corresponding to a 0.11 mg/dL decrease in phosphorus ($P = 0.003$; **Fig. 3E**). These alterations in neurotoxicity indices occur in the range of clinically significant hypophosphatemia. Moreover, the relationship between phosphorus and both ICANS and CARTOX-10 weakened with increasing time post-infusion, implicating the metabolically active infusion product as an important driver of changes in serum phosphorus and neurotoxicity indices.

We compared ICANS severity and duration in patients who did and did not experience hypophosphatemia. There was no significant difference in the grade of ICANS severity between these two (2.6 vs. 2.0, $P = 0.57$, Mann–Whitney U test). However, we did observe a significant difference in duration of ICANS in patients with hypophosphatemia compared with those without hypophosphatemia (mean duration 6.5 days vs. 1.0 days, $P = 0.008$, Mann–Whitney U test). In addition, we ran a logistic regression model with ICANS as the

Table 1. Demographics and outcomes of patients with and without ICANS after CD19-targeted CAR T-cell therapy.

		ICANS ($n = 23$)	No ICANS ($n = 54$)	*P*
Age, y		66.35	58.73	0.1787
Sex	M	12 (52%)	33 (61%)	0.6140
	F	11 (48%)	21 (39%)	
Diagnosis	NHL	21 (91%)	48 (89%)	1
	ALL	2 (7%)	6 (11%)	
Infusion product	Axicabtagene ciloleucel	21 (91%)	41 (76%)	0.2071
	Tisagenlecleucel	2 (9%)	13 (24%)	
CRS	Yes	23 (100%)	30 (56%)	<0.0001
	No	0 (0%)	24 (44%)	
Hypophosphatemia (Nadir < 2)		21/23 (91%)	25/54 (46%)	0.0003
Hypokalemia (Nadir < 3.5)		13/23 (56%)	27/54 (50%)	0.6276
Hypomagnesemia (Nadir < 1.6)		18/23 (78%)	38/54 (70%)	0.5823
Nadir phosphorus (mg/dL)		1.391 (0.896–1.886)	2.130 (1.285–2.975)	0.0002
Nadir potassium (mmol/L)		3.330 (3.018–3.643)	3.444 (3.143–3.745)	0.1421
Nadir magnesium (mg/dL)		1.413 (1.253–1.573)	1.450 (1.294–1.606)	0.3577
Peak CRP (mg/L)		8.887 (4.566–13.208)	4.585 (0.415–8.755)	<0.0001
Received dexamethasone		22/23 (96%)	5/54 (9%)	<0.0001
Received tocilizumab		20/23 (87%)	30/54 (56%)	0.0092
Received anakinra		7/23 (30%)	4/54 (7%)	0.0136
Response to therapy	CR	13/23 (57%)	31/54 (57%)	0.2701[a]
	PR	6/23 (26%)	5/54 (9%)	
	NR	4/23 (17%)	16/54 (30%)	
	Unknown[b]	0/23 (0%)	2/54 (4%)	

Note: For continuous variables, data are presented as mean and ± SD.
Abbreviations: F, female; M, male; NHL, Non-Hodgkin's lymphoma; CR, complete metabolic response; PR, partial response; NR, no response.
[a]Treatment response (CR+PR vs. NR).
[b]Patients declined posttreatment follow-up.

dependent variable and both severe CRS and hypophosphatemia as independent variables. We found that: (i) controlling for severe CRS, patients with hypophosphatemia had 1.9 times the odds of developing ICANS than did patients without hypophosphatemia, and (ii) controlling for hypophosphatemia, patients with severe CRS had 1.66 times the odds of developing ICANS than did patients without severe CRS (Supplementary Fig. S3). Although this is not a causal model, it does illustrate the associations between severe CRS and ICANS, as well as hypophosphatemia and ICANS, while controlling for hypophosphatemia and severe CRS, respectively.

Neither ICANS nor hypophosphatemia were associated with significant differences in treatment response PFS, or OS. In addition, the immune-suppressing agents used in the management of ICANS or CRS (tocilizumab, dexamethasone, and anakinra) were not associated with any significant difference in treatment response, PFS, or OS (all $P > 0.05$; Supplementary Fig. S4).

Discussion

Despite their clinical effectiveness, the serious side effects of CAR T-cell therapies often require escalation to an intensive care setting. ICANS affects approximately 50% of all CAR T-cell recipients (19). The need for biomarkers of ICANS represents an important area of potential improvement in these therapeutic protocols. Given the overlap in the neurologic symptoms of acute hypophosphatemia and ICANS (weakness, confusion, altered mental status, seizure, and coma), as well as the previously reported widespread incidence of hypophosphatemia in patients who have received CAR T-cell therapies or other adoptive cell therapeutics (2, 11, 12), we hypothesized that there could be an association between the sudden increase in metabolic demand driven by infused CAR T cells engaging with their target antigen and extracellular phosphorus depletion. Our data demonstrate a consistent association between hypophosphatemia and ICANS incidence and severity, as well as mechanistic *in vitro* evidence of direct extracellular phosphate consumption by CAR T cells during a period of increased metabolic demand in the setting of antigen-driven cytotoxic activity.

Previous studies have shown that sufficiently metabolically active systemic states (e.g., sepsis and its accompanying systemic inflammatory state) can be potent drivers of hypophosphatemia (13–15). Our clinical data showed that systemic inflammation is also significantly higher in patients who develop ICANS (as measured by overall incidence of CRS and peak CRP metrics). Therefore, it is likely that, in clinical settings of CAR T-cell infusion, the development of hypophosphatemia may be multifactorial due to systemic inflammation mediated by the CAR T-cell infusion as well as direct extracellular phosphorus consumption by the CAR T cells themselves.

Our metabolic assays showed greater baseline metabolic activity of T cells expressing the CD28 construct, consistent with previously published data (20), although this trend has been shown to diminish over time in favor of greater glycolysis metabolism. The authors of the previous study (20), concluded that metabolism driven by CD28 transmembrane CARs is somehow skewed towards glycolytic metabolism as opposed to that driven by 4–1BB CARs, which rely more heavily on ETC respiration. This observation, together with our data concerning phosphate consumption, indicates that glycolysis or ETC-focused CAR T-cell metabolisms still depletes phosphate

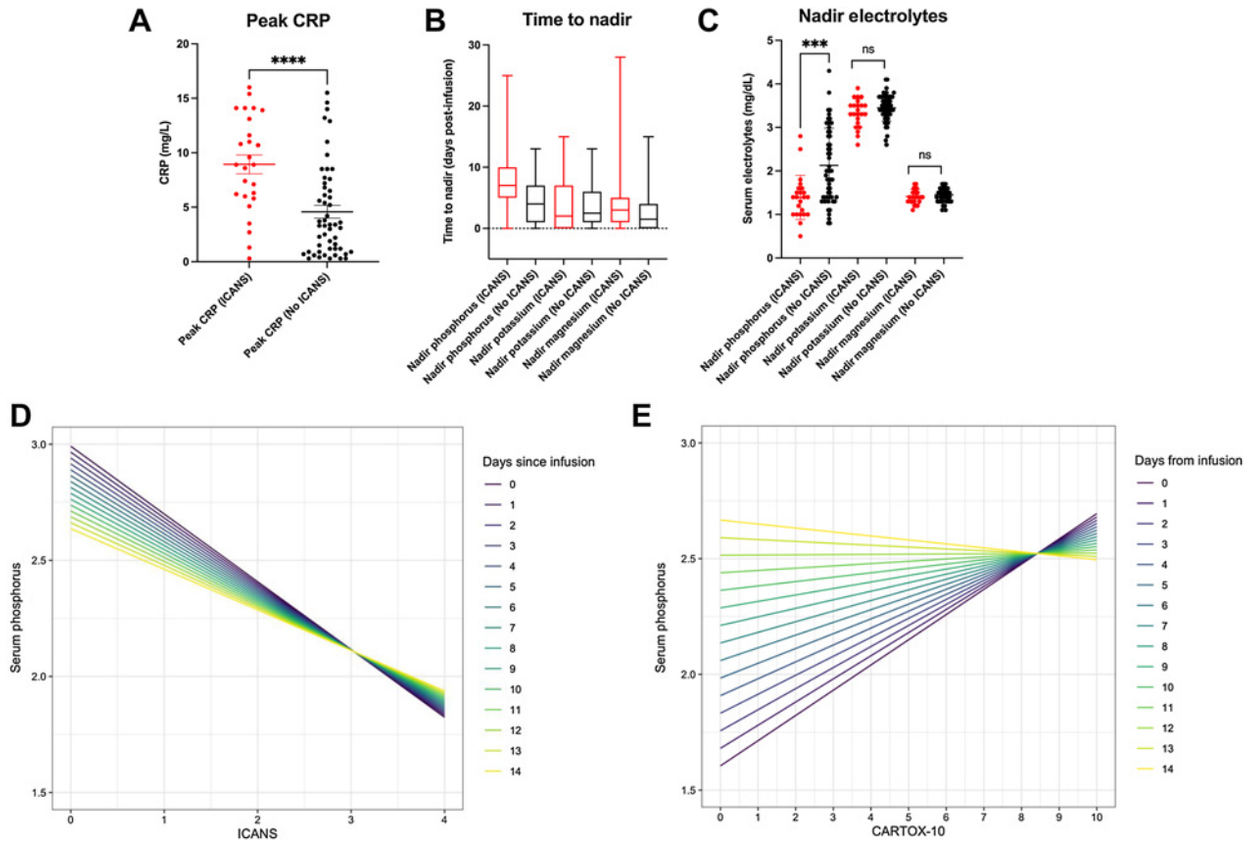

Figure 3.

Nadir serum phosphorus values and peak CRP values differ in patients who developed ICANS, and the severity of neurotoxicity is correlated with serum phosphorus within hypophosphatemic range, the strength of which depends on time from CAR T-cell infusion. **A,** Peak CRP values measured throughout admission in patients receiving CAR T-cell therapy who developed ICANS compared with those who did not (***, $P < 0.0001$; unpaired *t* test) represented as mean ± SEM. **B,** Time to nadir measured from days post CAR T-cell infusion represented as a box and whisker plot showing mean and range. **C,** Nadir serum phosphorus, potassium, and magnesium values measured throughout admission in patients receiving CAR T-cell therapy who developed ICANS compared with those who did not (***, $P < 0.0001$; unpaired *t* test) represented as mean ± SEM. **D,** Linear mixed-effects model with phosphorus as the outcome variable, and time from CAR T-cell infusion, as well as either ICANS or (**E**) CARTOX-10 as the fixed effect of the model. ICANS grades neurotoxicity from 1 to 4 with increasing severity of symptoms (with highest severity being 4), while a CARTOX-10 grades neurotoxicity from 1 to 10 with decreasing severity of symptoms (with lowest severity a 10). The color-coded lines represent the relationship between serum phosphorus and ICANS grade or CARTOX-10 as a function of time post-infusion.

extracellularly when exposed to antigen, whereas CD28 CARs simply require more baseline O_2 for their homeostasis. In addition, previous meta-analyses have shown that CD19-targeted CAR T-cell products bearing the CD28 construct are more strongly associated with incidence of ICANS (21). Further studies will be vital to determine the differential metabolic kinetics driven by various CAR T-cell constructs *in vivo*, and how these affect clinical outcomes and electrolyte derangements in patients. Indeed, the identification of factors responsible for certain drivers of CAR T-cell metabolism may be of value in the design of future generations of these therapeutics.

Our study has several limitations. Although our institutional SOPs listed above largely standardized electrolyte repletion protocols in the patients, these can vary from institution to institution, as well as being dependent on varying degrees of clinician discretion for more conservative repletion strategies. There may be additional confounders in the associations between both CRS and hypophosphatemia, and ICANS, such as potential renal dysfunction and the development of malnutrition during admission for CAR T-cell therapy, which would require larger meta-analyses to adequately elucidate beyond our single-institution experience. Although our study demonstrates correlation between hypophosphatemia and ICANS incidence and severity in CD19-targeted CAR T-cell therapy, further studies are needed to explore whether there is any causative mechanism for this phenomenon in the development of ICANS. Such an association would also be valuable to clinicians, as phosphate repletions are inexpensive, widely available, and have been well studied in other contexts of clinical hypophosphatemia (22). Future studies with *in vivo* models and prospective interventional clinical protocols will be required to explore this phenomenon.

In conclusion, we have demonstrated that *in vitro* CAR T-cell effector activity is associated with increased consumption of extracellular phosphorus, which is temporally associated with increased cytokinetic functionality and increased phosphorus-dependent metabolic demand of the CAR T cells. In a clinical setting, decreases in patient serum phosphorus levels correlated with the incidence and severity of ICANS. These results have implications for monitoring for the development of ICANS in the growing number of patients receiving adoptive cell therapies for cancer.

Authors' Disclosures

R.E. Yamada reports other support from Jaime Erin Follicular Lymphoma Research Consortium during the conduct of the study. J.M. Timmerman reports other support from Jamie Erin Follicular Lymphoma Research Consortium during the conduct of the study; grants from Kite Pharma outside the submitted work. T.S. Nowicki reports personal fees from Adaptive Biotechnologies; personal fees from PACT Pharma; and personal fees from Allogene Therapeutics outside the submitted work. No disclosures were reported by the other authors.

Disclaimer

The contents of this article are solely the responsibility of the authors and do not necessarily represent the official view of the NIH or the NCI.

Authors' Contributions

J.P. Tang: Conceptualization, formal analysis, investigation, visualization, methodology, writing–original draft, writing–review and editing. **C.W. Peters:** Conceptualization, formal analysis, validation, investigation, visualization, methodology, writing–original draft, writing–review and editing. **C. Quiros:** Formal analysis, investigation, visualization, methodology, writing–original draft, writing–review and editing. **X. Wang:** Formal analysis, investigation, visualization, methodology, writing–original draft. **A.M. Klomhaus:** Formal analysis, investigation, visualization, methodology, writing–original draft. **R.E. Yamada:** Methodology, writing–review and editing. **J.M. Timmerman:** Conceptualization, investigation, visualization, methodology, writing–review and editing. **T.B. Moore:** Investigation, visualization, methodology, writing–review and editing. **T.S. Nowicki:** Conceptualization, resources, data curation, software, formal analysis, supervision, funding acquisition, validation, investigation, visualization, methodology, writing–original draft, project administration, writing–review and editing.

Acknowledgments

We gratefully acknowledge Linsey Stiles and the UCLA Mitochondria and Metabolism Core for assistance with the Seahorse respirometry assays.

T.S. Nowicki is supported by the NIH grant K08 CA241088, as well as intramural funding from the UCLA CTSI, Jonsson Comprehensive Cancer Center, and the Eli and Edythe Broad Center for Regenerative Medicine and Stem Cell Research at UCLA. J.M. Timmerman is supported by the Jaime Erin Follicular Lymphoma Research Consortium.

Note

Supplementary data for this article are available at Cancer Immunology Research Online (http://cancerimmunolres.aacrjournals.org/).

Received May 24, 2022; revised July 27, 2022; accepted September 15, 2022; published first October 19, 2022.

References

1. June CH, Sadelain M. Chimeric antigen receptor therapy. N Engl J Med 2018;379:64–73.
2. Maude SL, Laetsch TW, Buechner J, Rives S, Boyer M, Bittencourt H, et al. Tisagenlecleucel in children and young adults with B-cell lymphoblastic leukemia. N Engl J Med 2018;378:439–48.
3. Neelapu SS, Locke FL, Bartlett NL, Lekakis LJ, Miklos DB, Jacobson CA, et al. Axicabtagene ciloleucel CAR T-cell therapy in refractory large B-cell lymphoma. N Engl J Med 2017;377:2531–44.
4. Neelapu SS, Tummala S, Kebriaei P, Wierda W, Gutierrez C, Locke FL, et al. Chimeric antigen receptor T-cell therapy—assessment and management of toxicities. Nat Rev Clin Oncol 2018;15:47–62.
5. Santomasso BD, Park JH, Salloum D, Riviere I, Flynn J, Mead E, et al. Clinical and biological correlates of neurotoxicity associated with CAR T-cell therapy in patients with B-cell acute lymphoblastic leukemia. Cancer Discov 2018;8:958–71.
6. Mehta P, Cron RQ, Hartwell J, Manson JJ, Tattersall RS, et al. Silencing the cytokine storm: the use of intravenous anakinra in haemophagocytic lymphohistiocytosis or macrophage activation syndrome. Lancet Rheumatol 2020;2:e358–67.
7. Liu S, Deng B, Yin Z, Pan J, Lin Y, Ling Z, et al. Corticosteroids do not influence the efficacy and kinetics of CAR T cells for B-cell acute lymphoblastic leukemia. Blood Cancer J 2020;10:15.
8. Lee DW, Gardner R, Porter DL, Louis CU, Ahmed N, Jensen M, et al. Current concepts in the diagnosis and management of cytokine release syndrome. Blood 2014;124:188–95.
9. Brentjens RJ, Davila ML, Riviere I, Park J, Wang X, Cowell LG, et al. CD19-targeted T cells rapidly induce molecular remissions in adults with chemotherapy-refractory acute lymphoblastic leukemia. Sci Transl Med 2013;5:177ra138.
10. Davila ML, Riviere I, Wang X, Bartido S, Park J, Curran K, et al. Efficacy and toxicity management of 19–28z CAR T-cell therapy in B-cell acute lymphoblastic leukemia. Sci Transl Med 2014;6:224ra225.
11. Gupta S, Seethapathy H, Strohbehn IA, Frigault MJ, O'Donnell EK, Jacobson CA, et al. Acute kidney injury and electrolyte abnormalities after chimeric antigen receptor T-cell (CAR T) therapy for diffuse large B-cell lymphoma. Am J Kidney Dis 2020;76:63–71.
12. D'Angelo SP, Melchiori L, Merchant MS, Bernstein D, Glod J, Kaplan R, et al. Antitumor activity associated with prolonged persistence of adoptively transferred NY-ESO-1 (c259)T cells in synovial sarcoma. Cancer Discov 2018;8:944–57.
13. Diringer M. Neurologic manifestations of major electrolyte abnormalities. Handb Clin Neurol 2017;141:705–13.
14. Marinella MA. The refeeding syndrome and hypophosphatemia. Nutr Rev 2003;61:320–3.
15. Shor R, Halabe A, Rishver S, Tilis Y, Matas Z, Fux A, et al. Severe hypophosphatemia in sepsis as a mortality predictor. Ann Clin Lab Sci 2006;36:67–72.
16. Divakaruni AS, Wallace M, Buren C, Martyniuk K, Andreyev AY, Li E, et al. Inhibition of the mitochondrial pyruvate carrier protects from excitotoxic neuronal death. J Cell Biol 2017;216:1091–105.
17. Ma C, Cheung AF, Chodon T, Koya RC, Wu Z, Ng C, et al. Multifunctional T-cell analyses to study response and progression in adoptive cell transfer immunotherapy. Cancer Discov 2013;3:418–29.
18. Rossi J, Paczkowski P, Shen YW, Morse K, Flynn B, Kaiser A, et al. Preinfusion polyfunctional anti-CD19 chimeric antigen receptor T cells are associated with clinical outcomes in NHL. Blood 2018;132:804–14.
19. Lee DW, Santomasso BD, Locke FL, Ghobadi A, Turtle CJ, Brudno JN, et al. ASTCT consensus grading for cytokine release syndrome and neurologic toxicity associated with immune effector cells. Biol Blood Marrow Transplant 2019;25:625–38.
20. Kawalekar OU, O'Connor RS, Fraietta JA, Guo L, McGettigan SE, Posey AD Jr, et al. Distinct signaling of coreceptors regulates specific metabolism pathways and impacts memory development in CAR T cells. Immunity 2016;44:712.
21. Meng J, Wu X, Sun Z, Xun R, Liu M, Hu R, et al. Efficacy and safety of CAR T-cell products axicabtagene ciloleucel, tisagenlecleucel, and lisocabtagene maraleucel for the treatment of hematologic malignancies: a systematic review and meta-analysis. Front Oncol 2021;11:698607.
22. Garber AK, Cheng J, Accurso EC, Adams SH, Buckelew SM, Kapphahn CJ, et al. Short-term outcomes of the study of refeeding to optimize inpatient gains for patients with anorexia nervosa: a multicenter randomized clinical trial. JAMA Pediatr 2021;175:19–27.